haematologica
Journal of the Ferrata Storti Foundation

Polytypic B cells, monotypic/monoclonal B-cell proliferations, and neoplastic T cells diverge from *TET2-/DNMT3A*-mutant clonal hematopoiesis in follicular helper T-cell lymphomas

by Natasha E. Lewis, Kseniya Petrova-Drus, Rohan Sardana, Sarah Huet, Qi Gao, Shenon Sethi, Chad Vanderbilt, Wenbin Xiao, Mikhail Roshal, Jeeyeon Baik, Himanshu Bhurtel, Alison J. Moskowitz, Steven M. Horwitz, and Ahmet Dogan

Received: Jan 31, 2024.
Accepted: July 12, 2024.

Citation: Natasha E. Lewis, Kseniya Petrova-Drus, Rohan Sardana, Sarah Huet, Qi Gao, Shenon Sethi, Chad Vanderbilt, Wenbin Xiao, Mikhail Roshal, Jeeyeon Baik, Himanshu Bhurtel, Alison J. Moskowitz, Steven M. Horwitz, and Ahmet Dogan. Polytypic B cells, monotypic/monoclonal B-cell proliferations, and neoplastic T cells diverge from TET2-/DNMT3A-mutant clonal hematopoiesis in follicular helper T-cell lymphomas.
Haematologica. 2024 July 18. doi: 10.3324/haematol.2024.285183 [Epub ahead of print]

Polytypic B cells, monotypic/monoclonal B-cell proliferations, and neoplastic T cells diverge from *TET2*-/*DNMT3A*-mutant clonal hematopoiesis in follicular helper T-cell lymphomas

Natasha E. Lewis[1*^], Kseniya Petrova-Drus[1,2*], Rohan Sardana[1], Sarah Huet[1#], Qi Gao[1], Shenon Sethi[1], Chad Vanderbilt[2], Wenbin Xiao[1], Mikhail Roshal[1], Jeeyeon Baik[1], Himanshu Bhurtel[1], Alison J. Moskowitz[3], Steven M. Horwitz[3], Ahmet Dogan[1]

[1]Hematopathology Service, Department of Pathology and Laboratory Medicine, Memorial Sloan Kettering Cancer Center, New York, NY, USA

[2]Diagnostic Molecular Pathology Service, Department of Pathology and Laboratory Medicine, Memorial Sloan Kettering Cancer Center, New York, NY, USA

[3]Lymphoma Service, Department of Medicine, Memorial Sloan Kettering Cancer Center, New York, NY, USA

*N.E.L. and K.P.-D. contributed equally as co-first authors

^Current affiliation: Division of Hematopathology, Department of Laboratory Medicine and Pathology, Mayo Clinic Arizona, Phoenix, AZ, USA

#Current affiliation: Laboratory of Haematology, CHU Lyon-Sud, Hospices Civils de Lyon, Pierre-Benite, France

Corresponding authors:

Natasha E. Lewis, MD, Department of Laboratory Medicine and Pathology, Mayo Clinic Arizona, 5777 E. Mayo Blvd, Phoenix, AZ, 85054; Phone: 480-574-5016; Email: lewis.natasha@mayo.edu, natashaelewis@gmail.com

Ahmet Dogan, MD, PhD, Department of Pathology and Laboratory Medicine, Memorial Sloan Kettering Cancer Center, 1275 York Ave, New York, NY, 10065; Phone: 212-639-5905; Email: dogana@mskcc.org

Running title: PolyBCs, MBPs, and TFHLs diverge from CH

Data Sharing: Data is available upon request from the corresponding authors.

Acknowledgements: Dr. Paul Grogan assisted with figure design.

Funding: This work was supported in part through the NIH/NCI Cancer Center Support Grant P30 CA008748, NIH/NCI MSK Lymphoma SPORE P50 CA192937 (A.D.), and NIH/NCI grant K08CA267058 (W.X.).

Authorship: N.E.L, K.P.-D., R.S., and A.D. conceived the study, collected and analyzed the data, and wrote the manuscript. K.P.-D. also annotated the sequencing data. C.V., S.H., S.S., J.B., and H.B. collected data. Q.G. and M.R. aided with flow cytometric analyses and flow cytometry cell sorting. A.J.M. and S.M.H. provided critical clinical information. W.X. and M.R. analyzed data and provided critical guidance.

Disclosures: N.E.L. consults and is on an advisory board for United States Drug Testing Laboratories. W.X. has received research support from Stemline Therapeutics. A.J.M. has received research support from Beigene, Seattle Genetics, Merck, Bristol-Myers Squibb, Incyte,

Affimed, and Astra-Zeneca and honoraria from Affimed, Merck, Seattle Genetics, and Takeda. S.M.H. has received research support from ADC Therapeutics, Affimed, C4, Celgene, Crispr Therapeutics, Daiichi Sankyo, Dren Kyowa Hakko Kirin, Millennium/Takeda, Seattle Genetics, and SecuraBio and honoraria from Affimed, Abcuro Inc, Corvus, Daiichi Sankyo, Kyowa Hakko Kirin, ONO Pharmaceuticals, SeaGen, SecuraBio, Takeda, and Yingli Pharmaceuticals. A.D. has received research support from Roche/Genentech, Takeda, and Astra-Zeneca. The remaining authors declare no competing financial interests related to this work.

Follicular helper T-cell lymphomas (TFHLs) frequently develop upon a background of *TET2*-/*DNMT3A*-mutant clonal hematopoiesis (CH)[1]. Monotypic/monoclonal B cell proliferations (MBPs), which are often, but not invariably, Epstein-Barr virus-positive (EBV+), commonly complicate TFHLs[2–5]. While rare reports found B cells can share *TET2*/*DNMT3A* mutations with TFHLs[6,7], MBP pathogenesis is incompletely understood. Here, we assessed mutational profiles of paired TFHLs and polytypic B cells (PolyBCs) or MBPs in the context of EBV status in 25 TFHL patients.

Cases with sufficient tissue for sequencing from both a TFHL and either PolyBCs or an MBP were genotyped utilizing targeted next-generation sequencing or, in select cases (n=4), droplet digital polymerase chain reaction as previously described[1] on bulk samples or flow cytometry (FC)-sorted cells, including T-, B-, and myeloid, as available (Supplemental Table 1), with an allele frequency (VAF) cut-off of >0.02. In bulk samples, mutant VAFs and percentages of cell types were compared to determine the cellular compartment in which a variant was present (see Supplemental Table 1 for details). The study was approved by the Memorial Sloan Kettering Institutional Review Board.

First, we analyzed FC-sorted PolyBCs from 11 TFHL patients (median age 67 [range 38-81] years, 7:4 females:males). PolyBCs were immunophenotypically normal with polytypic light chain expression by high-resolution FC (sensitivity at least 0.01%) and, if available, lacked morphologic evidence of a B cell proliferation. PolyBCs were collected pre- (n=6) or post-TFHL-directed therapy (n=5) (Figure 1) and included 7 EBV+ and 3 EBV-negative (EBV-)

patients (1 unknown) (Figure 2). Two patients (1, 8) whose PolyBCs were obtained post-therapy had histories of MBPs, however, 0/11 PolyBC patients subsequently developed an MBP.

PolyBCs harbored identical mutations as corresponding TFHLs in 7/11 patients (64%), consisting of *TET2* (6/7) and *DNMT3A* (3/7) (median VAFs 0.11 [range 0.02 – 0.27] and 0.04 [range 0.03 – 0.49], respectively) (Figure 2, Supplemental Table 1). Only 1 PolyBC sample (9% of total, 14% [1/7] of samples genotyped by next-generation sequencing) harbored a private mutation absent in its TFHL (patient 2, *TET2*). The incidence of shared mutations in PolyBCs and TFHLs was not significantly different among EBV+ and EBV- patients or among those with PolyBCs sampled pre- and post-treatment (Supplemental Figures 1A, 1B). *TET2*/*DNMT3A* mutant VAFs in PolyBCs did not differ among EBV+ and EBV- patients while a trend towards lower VAFs was present among pre-treatment samples (Supplemental Figures 1C, 1D). This suggests PolyBCs commonly arise from the same CH-harboring precursor as TFHLs, irrespective of EBV or treatment status, but uncommonly harbor private mutations.

Next, paired TFHLs and MBPs from 14 patients were evaluated (median age 74 [range 67-82] years, 3:11 females:males). MBPs were collected prior to (n=8) or following TFHL- or MBP-directed treatment (n=6) (Figure 1) and included large B-cell lymphoma (LBCL)-like (n=5), polymorphic (n=6), and follicular lymphoma-like (n=2) proliferations, and plasma cell myeloma (n=1) (Figures 2, 3A-S). Four of 5 LBCL-like, 6/6 polymorphic, and 1/2 follicular lymphoma-like proliferations were EBV+ (Figure 2).

Identical mutations within MBPs and TFHLs were identified in 9/14 patients (64%), consisting of *TET2* (9/9), *DNMT3A* (5/9), and *TET3* (1/9) (Figure 2, Supplemental Table 1). Additionally, 2 MBPs without shared mutations (CH-) harbored private *TET2* mutations, resulting in 11/14 (79%) MBPs exhibiting *TET2* and/or *DNMT3A* mutations in total (median VAFs 0.42 [range 0.10 – 0.56] and 0.27 [range 0.05 – 0.50], respectively). The shared *TET2*/*DNMT3A* mutant VAFs in MBPs were significantly higher than those in PolyBCs (Figure 3T). Twelve of 14 (86%) MBPs harbored private mutations absent in corresponding TFHLs (VAFs 0.10 - 0.99 [median 0.34]) (Figure 2, Supplemental Table 1), an incidence significantly higher than in PolyBCs (Figure 3U). Although few private mutations were recurrent, overall, they most affected signaling (n=22, e.g. *DTX1*, *KRAS*, *EPHA5*), epigenetic/transcriptional regulation (n=14, e.g. *TET2*, *KMT2D*, *SETD5*), and DNA damage response (n=3, e.g. *ATM*, *CHEK2*, *BRCA2*) genes. This suggests MBPs commonly arise from CH-harboring B cells but likely require additional genomic aberrations for transformation.

Neither the incidences of shared or private mutations nor the VAFs of shared mutations differed among EBV+ and EBV- or between pre- and post-treatment MBPs (Supplemental Figures 1E-J). The private mutant VAFs did not differ among EBV+ and EBV- or between CH+ and CH- MBPs (Supplemental Figures 1K, 1L). We saw no significant difference in the incidence of EBV positivity or of shared or private mutations or obvious difference in the types of private mutations among the MBP types (data not shown). CH mutations and EBV may thus not function in a mutually exclusive manner but may act separately or in concert to promote B cell survival and proliferation.

We also sequenced separate samples containing PolyBCs from 4 MBP patients (12, 15, 17, 19) (Supplemental Figure 2). Three samples with PolyBCs were genotyped in bulk, precluding assessment of shared mutations, however, none of them harbored the private mutations detected in the corresponding MBPs despite a high PolyBC content (20-35%) and high private mutant VAFs in the MBPs. The FC-sorted PolyBCs from patient 17 demonstrated the same *TET2* and *DNMT3A* mutations as those in their TFHL, MBP, and myeloid compartment, although at lower VAFs (all around 0.2 vs 0.47-0.50 in the MBP). They also harbored the MBP's private *TET2* and *PIK3C3* mutations, also at significantly lower VAFs (0.11 and 0.04 vs 0.48 and 0.52 in the MBP). This MBP shortly followed the PolyBC-containing sample (4.6 months). This supports that gain of private mutations occurs with MBP development and acquisition of certain private mutations may portend imminent transformation.

Myeloid compartments in 4/8 (50%) PolyBC and in 9/12 (75%) MBP patients shared *TET2* and/or *DNMT3A* mutations with PolyBCs and TFHLs (median VAFs 0.22 [range 0.06 – 0.47] and 0.26 [range 0.07 – 0.46]) and with MBPs and/or TFHLs (median VAFs 0.26 [range 0.05 – 0.97] and 0.14 [range 0.07 – 0.48]), respectively (Figure 2, Supplemental Table 1), supporting that the same CH-harboring precursor often gives rise to all 3 hematopoietic compartments in TFHL patients. The shared *TET2*/*DNMT3A* mutant VAFs did not differ between myeloid compartments of PolyBC and MBP patients (Figure 3V), suggesting the level of background CH may not predict MBP risk.

While proposed contributors to clonal B cell outgrowth in TFHL patients include latently EBV-infected B cell expansion due to defective immune surveillance and pro-proliferative properties

inherent in neoplastic TFH cells[5], contributions of genomic alterations were unknown. We show both PolyBCs and MBPs in TFHL patients often harbor EBV and share *TET2*/*DNMT3A* mutations with TFHLs, supporting origin from a common CH-harboring precursor. In contrast, private mutations are nearly exclusive to MBPs, which in conjunction with higher shared *TET2*/*DNMT3A* mutant VAFs than PolyBCs, suggest MBPs may arise from preferential outgrowth of pre-existing CH+ clones, which is driven by additional private alterations. Indeed, among 4 patients from whom both MBPs and PolyBCs were genotyped, only 1 harbored MBP-associated private mutations in PolyBCs with significantly lower VAFs. This clone's rapid growth and acquisition of an abnormal monotypic immunophenotype support that gain of such alterations may promote neoplastic progression. Thus, the multi-step model in which epigenetic dysregulation via *TET2*/*DNMT3A* mutations in premalignant hematopoietic precursors precedes lineage commitment and secondary alterations like that described in TFHLs and myeloid neoplasms[1,8] also likely applies to MBPs. While inclusion of post-treatment samples may have overestimated the incidence of shared mutations, as treatment may select for CH-harboring clones, the lack of significant difference in CH incidence among pre- and post-treatment samples in both PolyBC and MBP patients is reassuring. Nonetheless, this is a limitation of our study.

As CH and EBV positivity in B cells are detected more commonly than MBPs occur in TFHL patients (approximately 10%[2]), it is likely that neither is sufficient for MBP development without secondary private genomic alterations. Supporting this, our data showed no correlation between the incidence or level of CH-related or private mutations and EBV status in either PolyBCs or MBPs. However, given MBPs' relative frequency among TFHLs, this unique biology of CH mutations in B cells, EBV reactivation, and unchecked neoplastic TFH cell-mediated stimulation

may all increase MBP risk. One TFHL mouse model found *TET2* loss in all blood cells (including B cells) led to expansion of genomically aberrant B cells while *TET2* loss restricted to T cells did not, suggesting CH mutations in B cells may promote their proliferation and clonal expansion[9]. Additionally, our trend towards higher *TET2*/*DNMT3A* mutant VAFs in post-treatment PolyBCs suggests treatment could promote CH+ B cell outgrowth in a manner akin to therapy-related myeloid neoplasms. Larger studies would be needed to assess whether CH-derived B cells increase MBP risk.

Prior work demonstrated *NOTCH1* variants in microdissected B cells in 3/87 TFHLs[6]. While we interrogated *NOTCH1*, *NOTCH2*, *NOTCH3*, and *NOTCH4* in all 14 MBPs and in 7/11 PolyBCs, no mutations were found, possibly due to sample size. However, we detected missense variants in exons 1 and 2 of *DTX1* in 3/14 MPBs, which have been described in various B cell lymphomas[10–12]. DTX1 is a ubiquitin ligase that regulates NOTCH signaling and plays a role in B cell development[13]. Mutations in *DTX1* appear to hinder its ability to negatively regulate NOTCH signaling[11]. NOTCH pathway activation may thus be important in MBP development in TFHL patients, which can occur via alterations of multiple genes in the pathway.

Lastly, our data support that MBPs in TFHL patients are biologically unique. Compared to de novo EBV- LBCLs, EBV+ LBCLs more frequently harbor *TET2*/*DNMT3A* mutations and lack mutations common in activated B cell-type LBCLs (e.g.MYD88, CD79B)[14], similar to our results, suggesting a distinct pathogenesis and potential cooperation between EBV and CH mutations. Additionally, while LBCLs are typically aggressive and require intensive treatment,

we have observed MBPs in TFHL patients often favorably respond to anti-CD20 therapy alone, suggesting an individualized approach is warranted.

References

1. Lewis NE, Petrova-Drus K, Huet S, et al. Clonal hematopoiesis in angioimmunoblastic T-cell lymphoma with divergent evolution to myeloid neoplasms. Blood Adv. 2020;4(10):2261-2271.

2. Willenbrock K, Bräuninger A, Hansmann M-L. Frequent occurrence of B-cell lymphomas in angioimmunoblastic T-cell lymphoma and proliferation of Epstein-Barr virus-infected cells in early cases. Br J Haematol. 2007;138(6):733-739.

3. Balagué O, Martínez A, Colomo L, et al. Epstein-Barr virus negative clonal plasma cell proliferations and lymphomas in peripheral T-cell lymphomas: a phenomenon with distinctive clinicopathologic features. Am J Surg Pathol. 2007;31(9):1310-1322.

4. Suefuji N, Niino D, Arakawa F, et al. Clinicopathological analysis of a composite lymphoma containing both T- and B-cell lymphomas. Pathol Int. 2012;62(10):690-698.

5. Zettl A, Lee S-S, Rüdiger T, et al. Epstein-Barr virus-associated B-cell lymphoproliferative disorders in angioimmunoblastic T-cell lymphoma and peripheral T-cell lymphoma, unspecified. Am J Clin Pathol. 2002;117(3):368-379.

6. Nguyen TB, Sakata-Yanagimoto M, Asabe Y, et al. Identification of cell-type-specific mutations in nodal T-cell lymphomas. Blood Cancer J. 2017;7(1):e516.

7. Schwartz FH, Cai Q, Fellmann E, et al. TET2 mutations in B cells of patients affected by angioimmunoblastic T-cell lymphoma. J Pathol. 2017;242(2):129-133.

8. Cortes JR, Ambesi-Impiombato A, Couronné L, et al. RHOA G17V induces T follicular helper cell specification and promotes lymphomagenesis. Cancer Cell. 2018;33(2):259-273.e7.

9. Fujisawa M, Nguyen TB, Abe Y, et al. Clonal germinal center B cells function as a niche for T-cell lymphoma. Blood. 2022;140(18):1937-1950.

10. Rossi D, Trifonov V, Fangazio M, et al. The coding genome of splenic marginal zone lymphoma: activation of NOTCH2 and other pathways regulating marginal zone development. J Exp Med. 2012;209(9):1537-1551.

11. de Miranda NFCC, Georgiou K, Chen L, et al. Exome sequencing reveals novel mutation targets in diffuse large B-cell lymphomas derived from Chinese patients. Blood. 2014;124(16):2544-2553.

12. Green MR, Kihira S, Liu CL, et al. Mutations in early follicular lymphoma progenitors are associated with suppressed antigen presentation. Proc Natl Acad Sci U S A. 2015;112(10):E1116-1125.

13. Wang L, Sun X, He J, Liu Z. Functions and molecular mechanisms of deltex family ubiquitin E3 ligases in development and disease. Front Cell Dev Biol. 2021;9:706997.

14. Li Y, Xu-Monette ZY, Abramson J, et al. EBV-positive DLBCL frequently harbors somatic mutations associated with clonal hematopoiesis of indeterminate potential. Blood Adv. 2023;7(7):1308-1311.

15. Petrova-Drus K, Quesada AE, Bowman AS, et al. Quantitative off-target detection of Epstein-Barr virus-derived DNA in routine molecular profiling of hematopoietic neoplasms by panel-based hybrid-capture next-generation sequencing. J Mol Diagn. 2022;24(1):69-78.

Figure Legends

Figure 1. Clinical time points and outcomes of 25 follicular helper T-cell lymphoma patients. Swimmer plot depicting time points at which samples from each patient were collected, systemic therapy was initiated, allogeneic stem cell transplant (alloSCT) occurred, and clinical outcomes. Each row depicts 1 patient and is indicated by patient identification number. Month 0 indicates time at which a follicular helper T-cell lymphoma (TFHL) or monotypic/monoclonal B cell proliferation (MBP) was initially diagnosed. Horizontal arrows indicate patients alive at last follow-up while a lack of an arrow indicates a deceased patient.

Figure 2. Mutational profiles of various cellular compartments and Epstein-Barr virus status of 25 follicular helper T-cell lymphoma patients. Oncoplot detailing mutations detected in follicular helper T-cell lymphomas (TFHLs), polytypic B cells (PolyBCs), monotypic/monoclonal B cell proliferations (MBPs), and myeloid compartments. Each column represents 1 patient, labeled with patient identification numbers, and the subcolumns indicate the cellular compartment in which a mutation was evaluated (T: TFHL, B: PolyBC/MBP, M: myeloid). Only select private mutations identified in TFHLs are included (e.g., *RHOA, IDH2*) (see Supplemental Table 1 for all identified mutations). Whether a given cell population was sorted by flow cytometry (FC) is detailed at the bottom and the Epstein-Barr virus (EBV) status of each patient at the time of PolyBC or MBP collection is indicated at the top. EBV positivity was called based on either i) in situ hybridization for EBV-encoded RNA (EBER) reactivity anywhere within tissue sections for PolyBC patients or within the majority of cells for MBPs, ii) detection of plasma EBV DNA by quantitative polymerase chain reaction analysis (PolyBC

patients only), or iii) off-target EBV reads of ≥10 by next-generation sequencing as previously described[15].

Figure 3. Morphologic and immunohistochemical features of monotypic/monoclonal B cell proliferations and comparisons between polytypic B cells and monotypic/monoclonal B cell proliferations. The large B-cell lymphoma-like and follicular lymphoma-like B cell proliferations as well as the plasma cell myeloma all fulfilled 2022 International Consensus Classification/5th edition World Health Organization criteria for diagnosis of diffuse large B-cell lymphoma, follicular lymphoma, and plasma cell myeloma, respectively. The polymorphic B cell proliferations showed atypical polymorphic morphology along with an abnormal B cell immunophenotype by flow cytometry and/or a clonal immunoglobulin heavy chain gene rearrangement. (A-E) Epstein-Barr virus (EBV)-positive large B-cell lymphoma-like proliferation from patient 13. (A-B) This pan-dermal cutaneous proliferation demonstrated vague nodules and sheets of large lymphoid cells with distinct nucleoli and extensive necrosis. The neoplastic cells lacked (C) CD3 expression and expressed (D) CD20 and (E) EBV LMP1. (F-L) EBV-positive polymorphic B cell proliferation from patient 20. (F) The lymph node was effaced by scattered small B cells, frequent plasmacytoid cells, plasma cells, and few large B cells in a background of scattered intermediate sized neoplastic T cells. (G) CD20 strongly labeled the B cells and weakly labeled the plasmacytoid cells while (H) CD79a highlighted B, plasmacytoid, and plasma cells. (I) CD138 highlighted plasma cells. The B lineage cells expressed (J) EBER and aberrantly lacked both (K) kappa and (L) lambda light chain expression. (M-S) Lymph node from patient 23 involved by an EBV-negative, grade 3B follicular lymphoma-like B cell proliferation with plasmacytoid differentiation. (M-N) It demonstrated nodules of intermediate to

large sized B cells with rounded nuclei with admixed apoptoses and mitoses in a background of increased vascularity, sclerosis, eosinophils, and small to intermediate sized neoplastic T cells. The B cells expressed (O) CD20, (P) BCL6, and (Q) partial, weak BCL2, and showed kappa light chain restriction with (R) kappa and (S) lambda immunostains. (T) The allele frequencies (VAFs) of shared *TET2*/*DNMT3A* mutations (present in both follicular helper T-cell lymphoma and B cells) were significantly higher in the monotypic/monoclonal B cell proliferations (MBPs) than in the polytypic B cells, (U) as was the incidence of private mutations. (V) The VAFs of shared *TET2*/*DNMT3A* mutations within the myeloid compartments (mutations present in myeloid and follicular helper T-cell lymphoma and/or B cells) did not significantly differ between polytypic B cell and MBP patients. In the analyses in (T) and (V), only the variant with the highest VAF was used from patients harboring multiple mutations in the same gene. Horizontal lines in (T) and (V) indicate medians; ns, not significant.

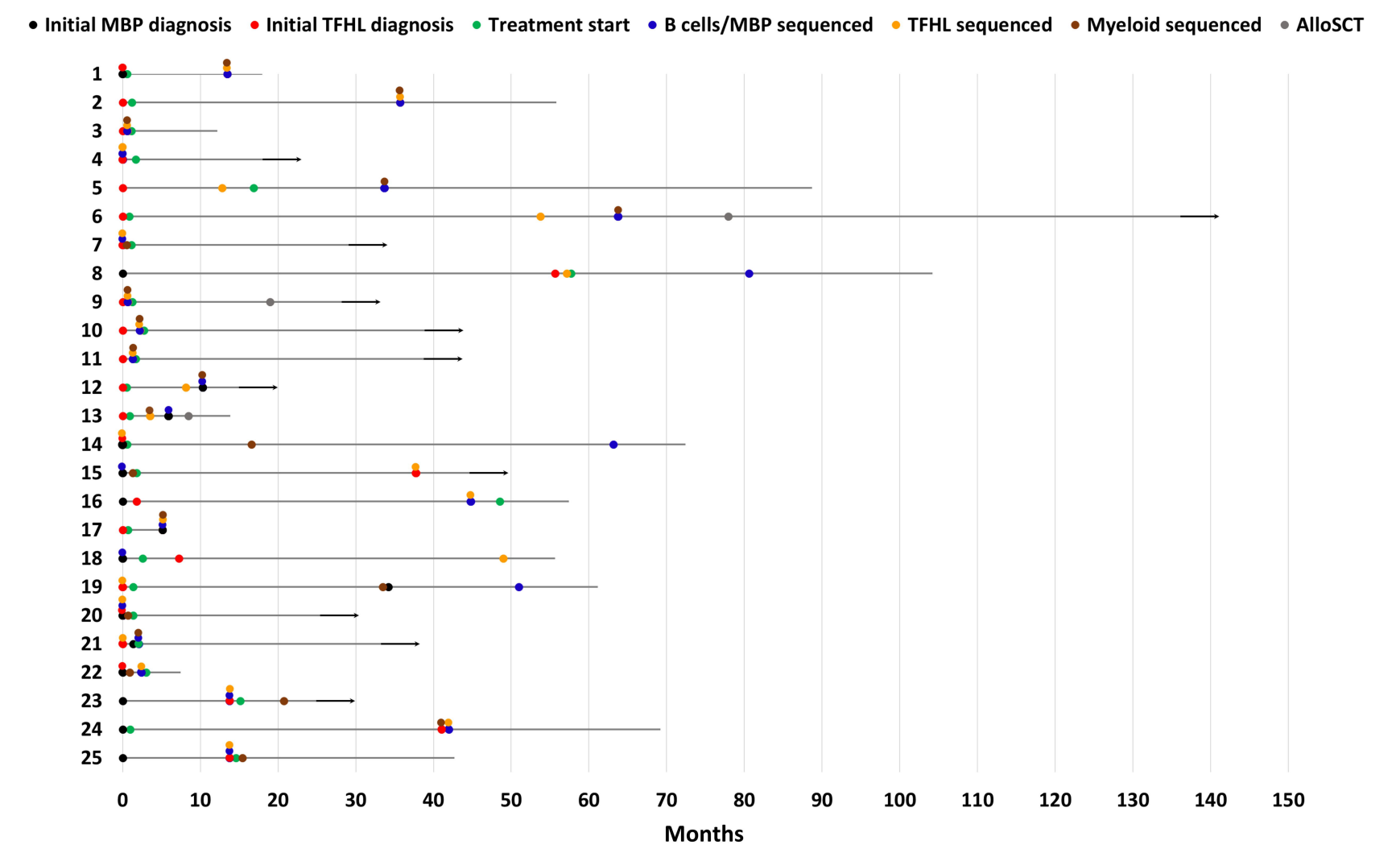
Initial MBP diagnosis
Initial TFHL diagnosis
Treatment start
B cells/MBP sequenced
TFHL sequenced
Myeloid sequenced
AlloSCT
1
2
3
4
5
6
7
8
9
10
11
12
13
14
15
16
17
18
19
20
21
22
23
24
25
0
10
20
30
40
50
60
70
80
90
100
110
120
130
140
150
Months

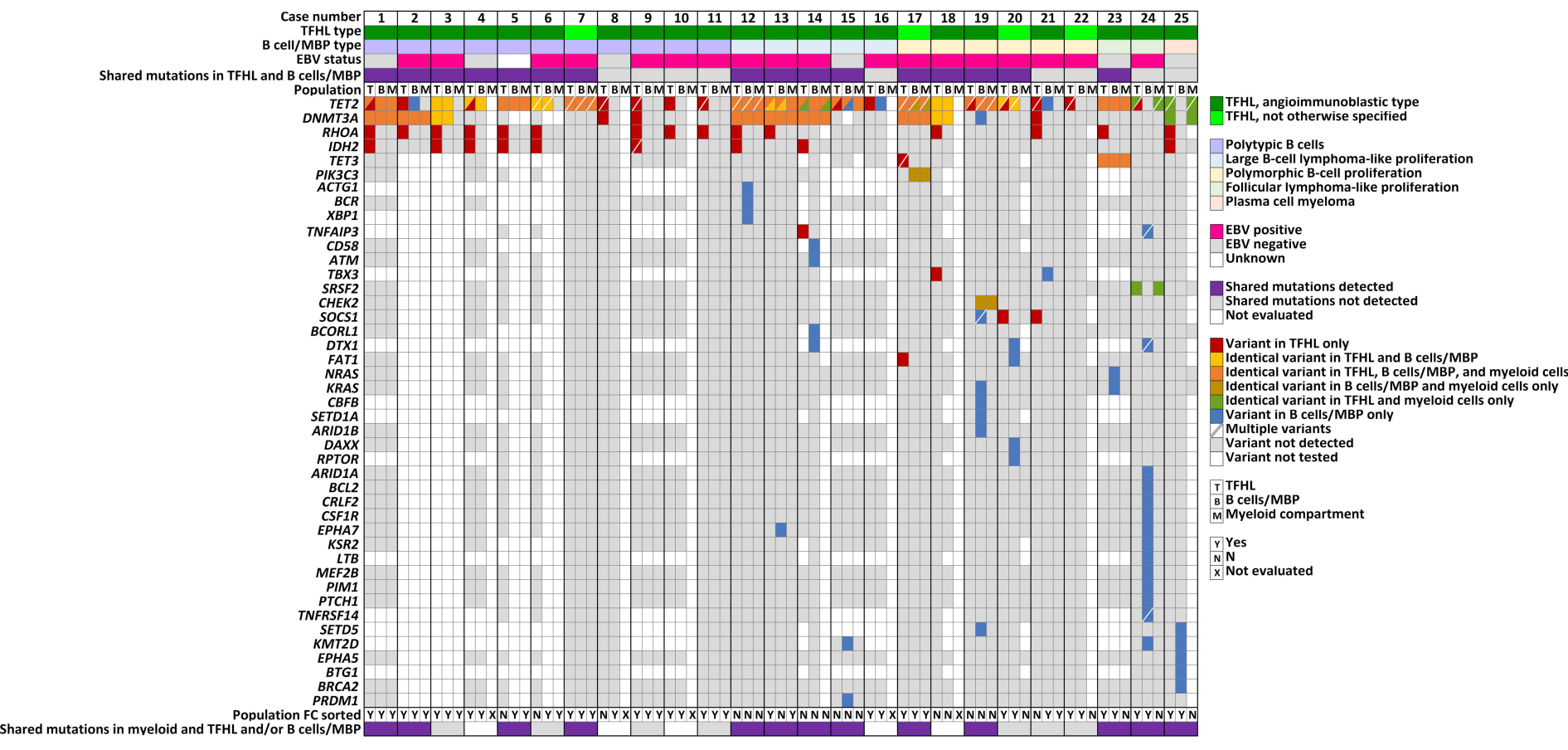
Case number
1 2 3 4 5 6 7 8 9 10 11 12 13 14 15 16 17 18 19 20 21 22 23 24 25
TFHL type
B cell/MBP type
EBV status
Shared mutations in TFHL and B cells/MBP
Population
T B M
TET2
DNMT3A
RHOA
IDH2
TET3
PIK3C3
ACTG1
BCR
XBP1
TNFAIP3
CD58
ATM
TBX3
SRSF2
CHEK2
SOCS1
BCORL1
DTX1
FAT1
NRAS
KRAS
CBFB
SETD1A
ARID1B
DAXX
RPTOR
ARID1A
BCL2
CRLF2
CSF1R
EPHA7
KSR2
LTB
MEF2B
PIM1
PTCH1
TNFRSF14
SETD5
KMT2D
EPHA5
BTG1
BRCA2
PRDM1
Population FC sorted
Y Y Y Y Y Y Y Y Y X N Y Y N Y Y Y Y N Y X Y Y Y Y Y X Y Y Y N N N Y N Y N N N N N N Y Y X Y Y Y N N X N N N Y Y N N Y Y Y Y N Y Y N Y Y N Y Y N
Shared mutations in myeloid and TFHL and/or B cells/MBP
TFHL, angioimmunoblastic type
TFHL, not otherwise specified
Polytypic B cells
Large B-cell lymphoma-like proliferation
Polymorphic B-cell proliferation
Follicular lymphoma-like proliferation
Plasma cell myeloma
EBV positive
EBV negative
Unknown
Shared mutations detected
Shared mutations not detected
Not evaluated
Variant in TFHL only
Identical variant in TFHL and B cells/MBP
Identical variant in TFHL, B cells/MBP, and myeloid cells
Identical variant in B cells/MBP and myeloid cells only
Identical variant in TFHL and myeloid cells only
Variant in B cells/MBP only
Multiple variants
Variant not detected
Variant not tested
T TFHL
B B cells/MBP
M Myeloid compartment
Y Yes
N N
X Not evaluated

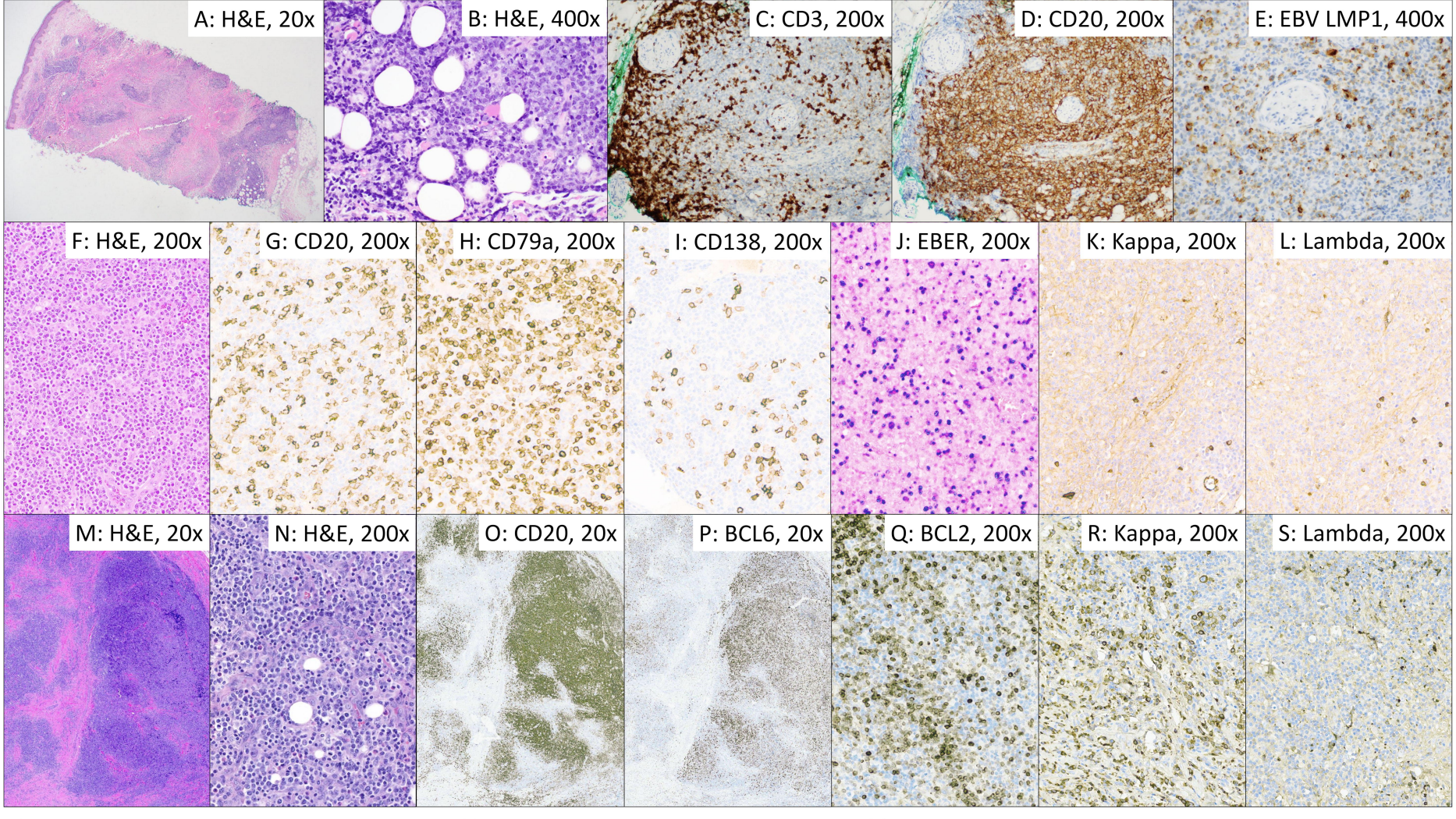
A: H&E, 20x
B: H&E, 400x
C: CD3, 200x
D: CD20, 200x
E: EBV LMP1, 400x
F: H&E, 200x
G: CD20, 200x
H: CD79a, 200x
I: CD138, 200x
J: EBER, 200x
K: Kappa, 200x
L: Lambda, 200x
M: H&E, 20x
N: H&E, 200x
O: CD20, 20x
P: BCL6, 20x
Q: BCL2, 200x
R: Kappa, 200x
S: Lambda, 200x

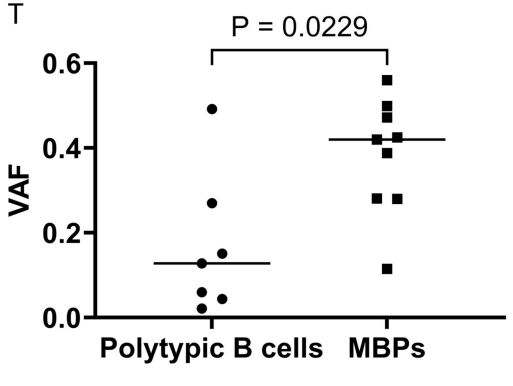
T
P = 0.0229
VAF
0.6
0.4
0.2
0.0
Polytypic B cells
MBPs

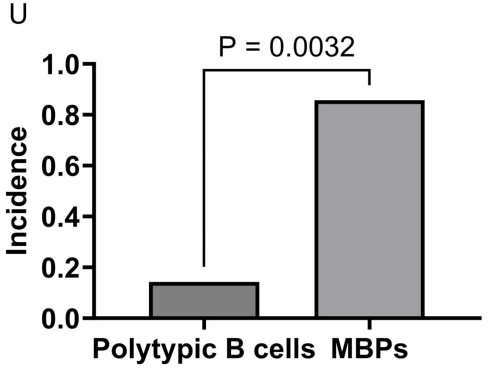
U
P = 0.0032
Incidence
1.0
0.8
0.6
0.4
0.2
0.0
Polytypic B cells
MBPs

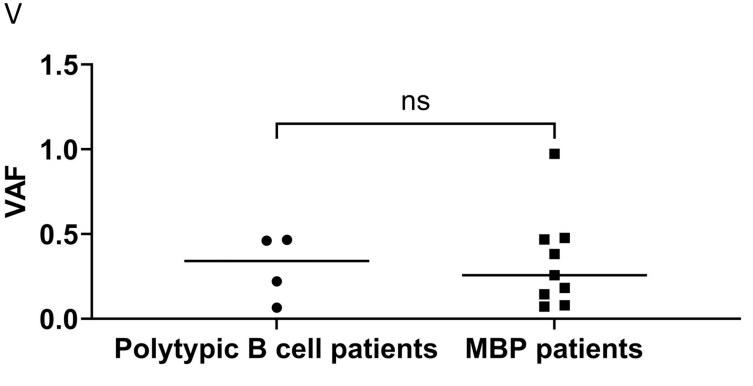
V
ns
VAF
1.5
1.0
0.5
0.0
Polytypic B cell patients
MBP patients

Polytypic B cells, monotypic/monoclonal B-cell proliferations, and neoplastic T cells diverge from *TET2*-/*DNMT3A*-mutant clonal hematopoiesis in follicular helper T-cell lymphomas

Natasha E. Lewis, Kseniya Petrova-Drus, Rohan Sardana, Sarah Huet, Qi Gao, Shenon Sethi, Chad Vanderbilt, Wenbin Xiao, Mikhail Roshal, Jeeyeon Baik, Himanshu Bhurtel, Alison J. Moskowitz, Steven M. Horwitz, Ahmet Dogan

Supplementary materials

Online Supplementary Table 1. Genomics of follicular helper T-cell lymphomas, polytypic B cells, monotypic/monoclonal B cell proliferations, and myeloid compartments in 25 follicular helper T-cell lymphoma patients

Online Supplementary Figure 1. Comparisons of the incidences and allele frequencies of shared and/or private mutations in polytypic B cells and monotypic/monoclonal B cell proliferations among various groups

Online Supplementary Figure 2. Comparison of mutations detected in samples containing high levels of polytypic B cells and monotypic/monoclonal B cell proliferations obtained from the same patients

Supplemental Table 1. Genomics of follicular helper T-cell lymphomas, polytypic B cells, monotypic/monoclonal B cell proliferations, and myeloid compartments in 25 follicular helper T-cell lymphoma patients

		T-Cell Lymphoma							B Cells/Monotypic/Monoclonal B Cell Proliferations								Myeloid Cells						
Patient	Variant	VAF	TCL Type	Genotyping Assay Utilized	Sample Type	Flow Sorted	Neoplastic T Cells in Sample	TCR Gene Rearrangement	VAF	B Cell Type	Genotyping Assay Utilized	EBV	Sample Type	Flow Sorted	Combined Myeloid and Neoplastic T Cells in Sample	IgH/TCR Gene Rearrangement (Method)	VAF	Myeloid Cell Type	Genotyping Assay Utilized	Sample Type	Flow Sorted	Combined B and Neoplastic T Cells in Sample	IgH/TCR Gene Rearrangement (Method)
1	DNMT3A p.R882H	0.52	TFHL-AI	MSK-IMPACT	BM	Y	NA	NT	0.49	Polytypic	MSK-IMPACT	Neg	BM	Y	NA	IgH: NT	0.46	Myeloid Cells	MSK-IMPACT	BM	Y	NA	NA
	TET2 p.M1333Nfs*6	0.49							0.10								0.06						
	TET2 p.G1145Vfs*7	0.45							0.00								0.00						
	RHOA p.G17L	0.51							0.00								0.00						
	IDH2 p.R172K	0.54							0.00								0.00						
2	DNMT3A p.W795C	0.49	TFHL-AI	ddPCR*	BM	Y	NA	Pos	0.04	Polytypic	ddPCR*	Pos	BM	Y	NA	IgH: NT	0.07	Monocytes	ddPCR*	BM	Y	NA	NA
	TET2 p.Y1337*	0.55							0.01								0.00						
	RHOA p.G17V	0.49							0.00								0.00						
	TET2 p.H1904Y	0.00							0.11								0.00						
3	TET2 p.Y592fs	0.51	TFHL-AI	ddPCR*	PB	Y	NA	Pos^	0.06	Polytypic	ddPCR*	Pos	PB	Y	NA	IgH: NT	0.01	Monocytes	ddPCR*	PB	Y	NA	NA
	DNMT3A exon11 splicing variant (c.1279+1G>A)	0.47							0.03								0.00						
	RHOA p.G17V	0.48							0.00								0.00						
	IDH2 p.R172K	0.49							0.00								0.00						
4	TET2 p.E1106Vfs*23	0.56	TFHL-AI	MSK-IMPACT	LN	Y	NA	NT	0.02	Polytypic	MSK-IMPACT	Neg	LN	Y	NA	IgH: NT	NT						
	TET2 p.S280*	0.44							0.00														
	RHOA p.G17V	0.46							0.00														
	IDH2 p.R172K	0.46							0.00														
5	TET2 p.P570fs	0.13	TFHL-AI	MSK-IMPACT	LN	N	10%	NT	0.15	Polytypic	ddPCR*	NA	PB	Y	NA	IgH: NT	0.22	Monocytes	ddPCR*	PB	Y	NA	NA
	RHOA p.G17V	0.06							0.00								0.00						
	IDH2 p.R172G	0.04							0.00								0.00						
	TET2 p.I873fs	0.06							NT								NT						
	PIK3CG p.V74M	0.13							NT								NT						
6	TET2 p.C973fs	0.07	TFHL-AI	MSK-IMPACT[#]	LN	N	10-15%	Pos	0.27	Polytypic	ddPCR*	Pos	PB	Y	NA	IgH: NT	0.00	Monocytes	ddPCR*	PB	Y	NA	NA
	TET2 p.R1216*	0.08							0.07								0.00						
	RHOA p.G17V	0.05							0.00								0.00						
	IDH2 p.R172S	0.06							0.00								0.00						
7	TET2 N427Vfs*4	0.47	TFHL-NOS	MSK-IMPACT[#]	LN	Y	NA	Pos	0.13	Polytypic	MSK-IMPACT[#]	Pos	LN	Y	NA	IgH: NT	0.43	Granulocytes	MSK-IMPACT[#]	BM	Y	NA	NA
	TET2 X1268_splice	0.44							0.13								0.47						
	STAT5A p.N398K	0.47							0.00								0.00						
8	TET2 p.Q1537*	0.12	TFHL-AI	MSK-IMPACT[#]	LN	N	20%	Pos^	0.00	Polytypic	MSK-IMPACT[#]	Neg	LN	Y	NA	IgH: NT	NT						
	TET2 p.N1610Ifs*6	0.11							0.00														
	DNMT3A p.I681M	0.10							0.00														
	TP53 p.MA160IS	0.01							0.00														
9	TET2 p.M1656Ifs*36	0.44	TFHL-AI	MSK-IMPACT	LN	Y	NA	Pos	0.00	Polytypic	MSK-IMPACT	Pos	LN	Y	NA	IgH: NT	0.00	Granulocytes	MSK-IMPACT	PB	Y	NA	NA
	TET2 p.G1154D	0.30							0.00								0.00						
	DNMT3A p.C557*	0.46							0.00								0.00						
	RHOA p.G17V	0.46							0.00								0.00						
	IDH2 p.R172S	0.39							0.00								0.00						
	IDH2 p.R172S	0.07							0.00								0.00						
	CD28 p.T195P	0.41							0.01								0.00						
10	TET2 p.Q1539*	0.51	TFHL-AI	MSK-IMPACT	LN	Y	NA	Pos^	0.00	Polytypic	MSK-IMPACT	Pos	LN	Y	NA	IgH: NT	NT						
	RHOA p.G17V	0.51							0.00														
11	TET2 p.Q1138Kfs*14	0.48	TFHL-AI	MSK-IMPACT[#]	PB	Y	NA	NT	0.00	Polytypic	MSK-IMPACT[#]	Pos	PB	Y	NA	IgH: NT	0.00	Myeloid Cells	MSK-IMPACT[#]	PB	Y	NA	NA
	TET2 p.C1271Wfs*29	0.46							0.00								0.00						
	RHOA p.G17V	0.59							0.00								0.00						
	ARID5B p.E456Kfs*23	0.32							0.00								0.00						
	CDK12 p.I873dup	0.41							0.00								0.00						
12	TET2 p.Q778*	0.42	TFHL-AI	MSK-IMPACT[#]	LN	N	15%	NT	0.43	LBCL-like MBP	MSK-IMPACT[#]	Pos	GE junction	N	≤5%	IgH/TCR: NT	0.48	Bulk BM	MSK-IMPACT[#]	BM	N	≤5%	IgH/TCR: NT
	TET2 p.D1384N	0.28							0.41								0.45						
	DNMT3A p.V296M	0.41							0.39								0.48						
	RHOA p.G17V	0.07							0.00								0.00						
	IDH2 p.R172S	0.06							0.00								0.00						
	NCOR2 p.A989T	0.07							0.00								0.00						
	SETD1B p.E612*	0.05							0.00								0.00						
	XBP1 p.S52N	0.00							0.25								0.00						
	BCR p.G6D	0.00							0.25								0.00						
	ACTG1 p.S60T	0.00							0.22								0.00						
13	TET2 p.W1233*	0.31	TFHL-AI	MSK-IMPACT[#]	BM	Y	NA	Pos	0.28	LBCL-like MBP	MSK-IMPACT[#]	Pos	Skin	N	≤5%	IgH/TCR: NT	0.07	Myelomonocytic cells	MSK-IMPACT[#]	BM	Y	NA	NA
	TET2 p.Q674*	0.33							0.22								0.00						
	DNMT3A p.V872F	0.29							0.27								0.08						
	RHOA p.G17V	0.24							0.00								0.00						
	CTNNB1 p.G48C	0.32							0.01								0.00						
	CTNNB1 p.S45F	0.30							0.00								0.00						
	GRIN2A p.X336_splice	0.24							0.00								0.00						
	EPHA7 p.A816V	0.00							0.20								0.00						

14	TET2 p.N427fs	0.17	TFHL-AI	MSK-IMPACT[#]	LN	N	15%	Pos	0.10	LBCL-like MBP	MSK-IMPACT[#]	Pos	Skin/Subq	N	≤5%	IgH/TCR: NT	0.05	Bulk BM	28 gene panel	BM	N	≤1%	IgH and TCR: Neg (PCR)
	TET2 p.Q745X	0.16							0.09								0.06						
	DNMT3A p.M801V	0.21							0.12								0.14						
	IDH2 p.R172G	0.04							0.00								0.00						
	TNFAIP3 p.R271*	0.18							0.00								NT						
	PAK7 p.P442Q	0.12							0.00								NT						
	MED12 p.R1343S	0.08							0.00								NT						
	TSC2 p.P542L	0.08							0.00								NT						
	BRAF p.K601N	0.03							0.00								NT						
	ATM p.P2842T	0.00							0.10								NT						
	BCORL1 p.V866F	NT							0.10								NT						
	DTX1 p.A120T	NT							0.07								NT						
	CD58 p.P125Hfs*5	NT							0.05								NT						
15	TET2 p.Y1661*	0.44	TFHL-AI	MSK-IMPACT	LN	N	40%	Pos	0.42	LBCL-like MBP	MSK-IMPACT	Neg	Skin/Subq	N	≤10%	IgH/TCR: NT	0.38	Bulk PB	MSK-IMPACT	PB	N	≤5%	IgH/TCR: NT
	TET2 p.I1873T	0.22							0.03								0.00						
	TET2 p.T1554Sfs*16	0.11							0.06								0.00						
	PRDM1 p.Q171*	0.00							0.30								0.00						
	KMT2D p.S2910Rfs*32	0.00							0.25								0.00						
	TET2 p.N1746Kfs*5	0.00							0.23								0.00						
	SF3B1 p.K666N	0.00							0.00								0.05						
	TP53 p.H193R	0.00							0.00								0.03						
16	TET2 p.R1452*	0.85	TFHL-AI	MSK-IMPACT	PB	Y	NA	Neg^	0.00	LBCL-like MBP	MSK-IMPACT	Pos	PB[†]	Y	NA	IgH: NT	NT						
	TET2 p.L1276Wfs*87	0.00							0.45														
17	TET2 p.S631*	0.45	TFHL-NOS	MSK-IMPACT[#]	PB	Y	NA	Pos^	0.49	Polymorphic MBP	MSK-IMPACT[#]	Pos	PB[‡]	Y	NA	IgH: NT	0.11	Myeloid Cells	MSK-IMPACT[#]	PB	Y	NA	NA
	TET2 p.G641W	0.49							0.47								0.13						
	DNMT3A p.K455*	0.47							0.50								0.18						
	TET2 p.V1232Gfs*21	0.00							0.48								0.09						
	PIK3C3 p.S460P	0.00							0.52								0.09						
	TET3 p.C693G	0.52							0.00								0.00						
	TET3 p.C695Y	0.47							0.00								0.00						
	MAP2K1 p.K57N	0.08							0.00								0.00						
	MAP2K1 p.Q45_E62del	0.02							0.00								0.00						
	SPEN p.S147*	0.07							0.00								0.00						
	FAT1 M1?	0.08							0.00								0.00						
	CCND3 p.R271Pfs*53	0.27							0.00								0.00						
	HNF1A p.M154I	0.21							0.00								0.00						
	CHEK2 p.C284*	0.00							0.00								0.03						
	PTCH1 p.L39Cfs*41	0.00							0.00								0.03						
	TET2 p.Q1030*	0.00							0.00								0.01						
18	TET2 p.L1740*	0.38	TFHL-AI	MSK-IMPACT[#]	LN	N	10%	Pos	0.27	Polymorphic MBP	MSK-IMPACT	Pos	LN	N	≤10%	IgH: Pos (PCR, NGS)^, TCR: NT	NT						
	DNMT3A p.X518_splice	0.40							0.28														
	RHOA p.G17V	0.06							0.00														
	CTNNB1 p.S45F	0.06							0.00														
	TBX3 p.A280T	0.06							0.00														
19	TET2 p.S577Pfs*3	0.37	TFHL-AI	MSK-IMPACT[#]	LN	N	60%	Pos	0.39	Polymorphic MBP	MSK-IMPACT[#]	Pos	LN	N	≤10%	TCR: Neg (PCR), TCRg: Pos (NGS, 0.1%), IgH: NT	0.43	Bulk BM	MSK-IMPACT[#]	BM	N	≤1%	TCRg: Pos (NGS, 0.09%), IgH: NT
	TET2 p.F1300V	0.07							0.28								0.47						
	TET2 p.C1289F	0.24							0.02								0.00						
	CUX1 p.E555L	0.30							0.00								0.00						
	SETBP1 p.L1421P	0.30							0.00								0.00						
	VAV1 p.Y174C	0.33							0.00								0.00						
	CHEK2 p.D134G	0.02							0.28								0.44						
	CBFB p.I102F	0.00							0.14								0.00						
	KRAS p. A146T	0.00							0.13								0.01						
	SETD1A p.G444R	0.01							0.13								0.00						
	SETD5 p.A232V	0.00							0.12								0.00						
	SOCS1 p.NQ5K*	0.00							0.11								0.00						
	SOCS1 p.F79_Y80delinsLH	0.00							0.10								0.00						
	ARID1B p.G357dup	0.00							0.09								0.00						
	DNMT3A p.R736H	0.01							0.05								0.00						
	SRSF2 p.P95H	0.00							0.11								0.48						
	FBXO11 p.Y692H	0.01							0.09								0.44						
20	TET2 p.Q324Hfs*23	0.33	TFHL-NOS	MSK-IMPACT[#]	LN	Y	NA	Pos	0.47	Polymorphic MBP	MSK-IMPACT[#]	Pos	LN	Y	NA	IgH: Pos (PCR)	0.01	Bulk saliva and nails	MSK-IMPACT	Saliva and nails	N	NA	IgH/TCR: NT
	TET2 p.Q831*	0.38							0.46								0.00						
	SOCS1 p.R179P	0.37							0.00								0.00						
	TET2 p.L1276Sfs*22	0.05							0.00								0.00						
	DTX1 p.G58V	0.01							0.47								NT						
	FAT1 p.I1302M	0.00							0.15								0.00						
	DAXX p.F79L	0.00							0.09								0.00						
	RPTOR p.R616H	0.00							0.08								0.00						

21	TET2 p.A1373E	0.10	TFHL-AI	MSK-IMPACT[#]	LN	N	20%	NT	0.00	Polymorphic MBP	MSK-IMPACT[#]	Pos	PB[†]	Y	NA	IgH: NT	0.00	Granulocytes	MSK-IMPACT[#]	PB	Y	NA	NA
	TET2 p.V1136Cfs*6	0.06							0.00								0.00						
	DNMT3A p.P700L	0.10							0.00								0.00						
	RHOA p.G17V	0.09							0.00								0.00						
	CD28 p.T195P	0.10							0.00								0.00						
	SOCS1 p.I194N	0.08							0.00								0.00						
	PLCG1 p.D1169G	0.06							0.00								0.00						
	TET2 p.C1271*	0.00							0.38								0.00						
	TBX3 p.G218V	0.00							0.06								0.00						
22	TET2 p.H1382D (C>G)	0.45	TFHL-NOS	MSK-IMPACT[#]	LN	Y	NA	Pos^	0.00	Polymorphic MBP	MSK-IMPACT[#]	Pos	PB[†]	Y	NA	IgH: Pos (PCR)^	0.00	Bulk BM	49 gene panel	BM	N	≤5%	IgH: Pos (PCR), TCR: NT
	TET2 p.S1494* (C>A)	0.47							0.00								0.00						
23	TET2 p.Y1628*	0.40	TFHL-AI	MSK-IMPACT	LN	Y	NA	NT	0.56	FL-like MBP, grade 3B	MSK-IMPACT	Neg	LN	Y	NA	IgH: NT	0.97	Bulk BM	MSK-IMPACT	BM	N	≤5%	IgH and TCR: Neg (PCR)
	TET3 p.T35Sfs*45	0.21							0.32								0.47						
	RHOA p.G17V	0.14							0.00								0.00						
	KRAS p.A146V	0.01							0.26								0.06						
	NRAS p.G12V	0.00							0.10								0.09						
	ARID2 p.R13Efs*22	0.00							0.00								0.06						
24	TET2 p.R1400*	0.48	TFHL-AI	MSK-IMPACT[#]	LN	Y	NA	Pos	0.00	FL-like MBP, grade 3A	MSK-IMPACT[#]	Pos	LN	Y	NA	IgH: Neg (PCR)	0.26	Bulk saliva	MSK-IMPACT	Saliva	N	NA	IgH/TCR: NT
	SRSF2 p.P95H	0.46							0.00								0.36						
	TET2 p.R1465*	0.43							0.00								0.02						
	TET2 p.Q734*	0.04							0.00								0.00						
	ARID1A p.G105Efs*8	0.00							0.28								0.00						
	BCL2 p.E13D	0.00							0.43								0.00						
	CRLF2 p.C180Y	0.00							0.51								0.00						
	CSF1R p.V38L	0.00							0.39								0.00						
	DTX1 p.G58D	0.00							0.49								0.00						
	DTX1 p.V70L	0.01							0.52								0.00						
	EPHA7 p.I11N	0.00							0.52								0.00						
	KMT2D p.Q3961*	0.01							0.35								0.00						
	KSR2 p.S184I	0.00							0.46								0.00						
	LTB p.V36L	0.00							0.46								0.00						
	MEF2B p.D83V	0.00							0.99								0.00						
	PIM1 p.S75P	0.00							0.47								0.00						
	PTCH1 p.P299L	0.01							0.45								0.00						
	TNFAIP3 p.R136Qfs*3	0.02							0.34								0.00						
	TNFAIP3 p.L324Qfs*7	0.00							0.30								0.00						
	TNFRSF14 p.G60D	0.00							0.69								0.00						
	TNFRSF14 p.N116Rfs*117	0.00							0.18								0.00						
25	TET2 p.Y1128*	0.46	TFHL-AI	MSK-IMPACT[#]	BM	Y	NA	Pos	0.00	MM	MSK-IMPACT[#]	Neg	BM	Y	NA	IgH: Pos (PCR)	0.05	Bulk PB	49 gene panel	PB	N	≤1%	IgH/TCR: NT
	TET2 p.Q810*	0.46							0.00								0.05						
	DNMT3A p.R736C	0.48							0.00								0.07						
	RHOA p.G17V	0.46							0.00								NT						
	IDH2 p.R172K	0.41							0.00								0.00						
	ATR p.D1409N	0.21							0.00								NT						
	KMT2B p.Q757*	0.25							0.00								NT						
	BRCA2 p.A2306S	0.00							0.48								NT						
	BTG1 p.K29*	0.00							0.48								NT						
	EPHA5 p.G1033E	0.00							0.23								NT						
	KMT2D p.H1525Pfs*37	0.00							0.25								NT						
	SETD5 p.Y987F	0.00							0.35								NT						

Footnote: Targeted next-generation sequencing (NGS)-based mutational analysis was performed using Memorial Sloan Kettering laboratory-developed hybrid-capture-based 400 or 410 gene panels (MSK-IMPACT) with or without a matched germline control (minimum depth of coverage 100x) or microdroplet amplicon-based 28 or 49 gene panels (minimum depth of coverage 500x), all containing at least 28 genes commonly mutated in hematopoietic neoplasms. Mutations with allele frequencies (VAFs) ≤0.02 are included here but were not included in the final analysis. Percentages of neoplastic T-, total B-, and/or myeloid cells in a sample (based on morphology, immunohistochemistry, flow cytometry, and/or gene rearrangement analysis) are reported only for unsorted samples. Variants with VAFs >2x the percentage of neoplastic T- and myeloid cells combined in bulk monotypic/monoclonal B cell proliferation (MBP) samples and of neoplastic T- and total B cells in bulk blood (PB) or bone marrow (BM) samples were considered present in MBP or myeloid compartments, respectively, as variants at those levels would generally be too high to be explained by the T/myeloid or T/B cells alone and would most likely be present in the remaining compartment (MBP or myeloid, respectively). Clonality assessment was performed during clinical case work up using polymerase chain reaction (PCR)-based (T cell receptor [TCR] gamma [TCRg] and beta, immunoglobulin heavy chain [IgH]) and/or NGS-based (TCRg, IgH) gene rearrangement assays. IgH gene rearrangement results are reported on all polytypic B cell and MBP samples (to provide clonality evaluation) and on bulk myeloid samples (to provide sample purity evaluation). TCR gene rearrangement results are reported on T-cell lymphoma (TCL) samples (PCR only) (to provide clonality evaluation) and on bulk MBP and myeloid samples (to provide purity evaluation). For TCR gene rearrangement studies using NGS, the percentage indicates the percentage of clonal reads of all rearranged TCR reads. *Droplet digital polymerase chain reaction (ddPCR) was performed utilizing custom primers targeting mutated genes detected by targeted NGS performed on corresponding bulk TCL samples (see Figure 2 for genes evaluated). For patients 2 and 3, the targeted NGS was performed on a separate TCL sample (data not shown). ^Performed on a separate similar sample. [#]Matched germline control (nails or saliva) utilized. [†]The histologic type of MBP was determined on a concurrent or recent (obtained within 3 months) tissue sample that demonstrated the same B cell immunophenotype by flow cytometry and/or immunohistochemistry as the immunophenotypically abnormal B cell population identified in the genotyped PB sample by flow cytometry. [‡]Only a PB sample was available for evaluation, which showed an abnormal, light chain restricted B cell population with plasmacytic differentiation by flow cytometry and a lack of a significant population of large lymphocytes on the PB smear. EBV indicates Epstein-Barr virus; FL, follicular lymphoma; GE, gastroesophageal; LBCL, large B-cell lymphoma; LN, lymph node; MM, plasma cell myeloma; N, no; NA, not applicable; Neg, negative; NT, not tested; Pos, positive; TFHL-AI, follicular helper T-cell lymphoma, angioimmunoblastic type; TFHL-NOS, follicular helper T-cell lymphoma, not otherwise specified; Subq, subcutaneous tissue; Y, yes.

Supplemental Figure 1

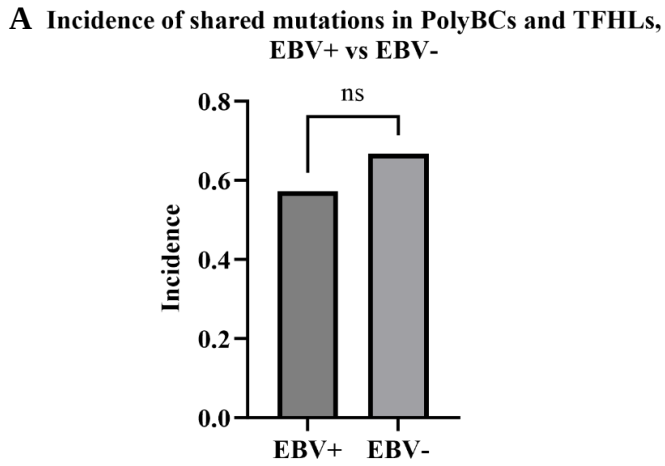

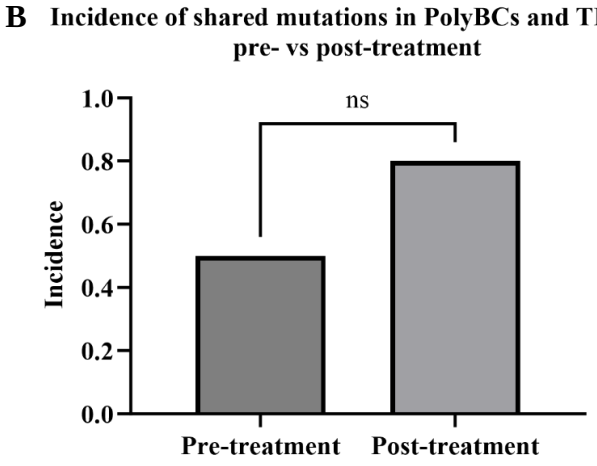

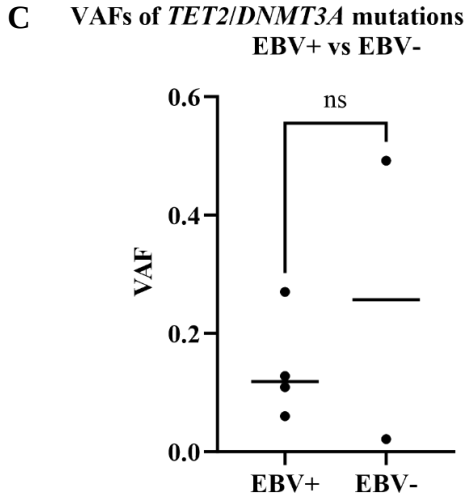

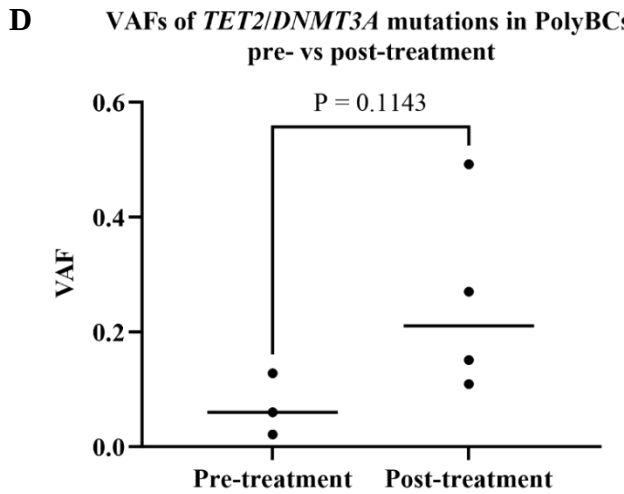

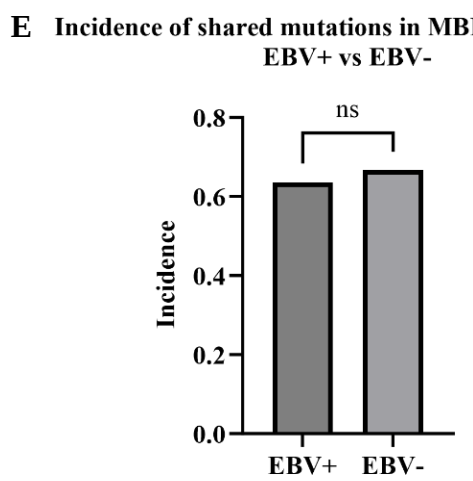

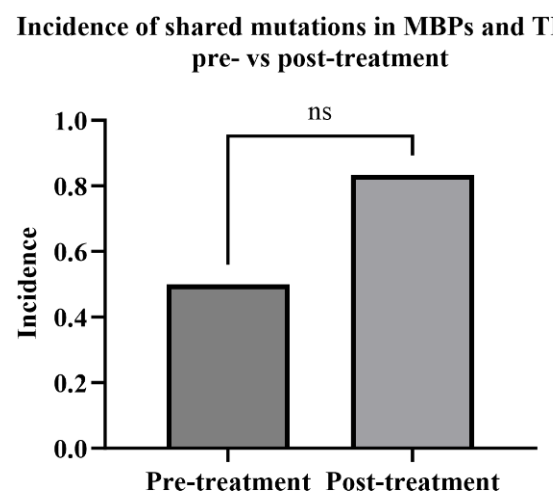

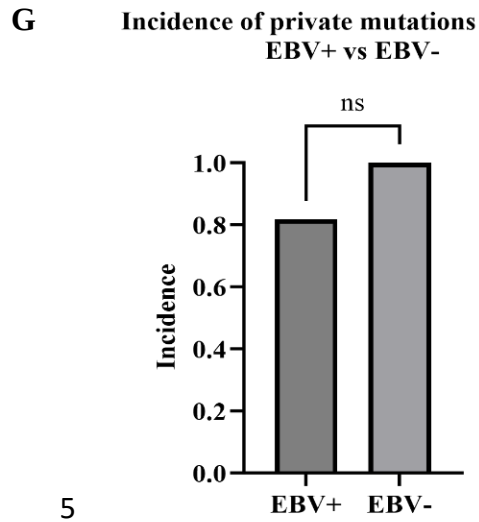

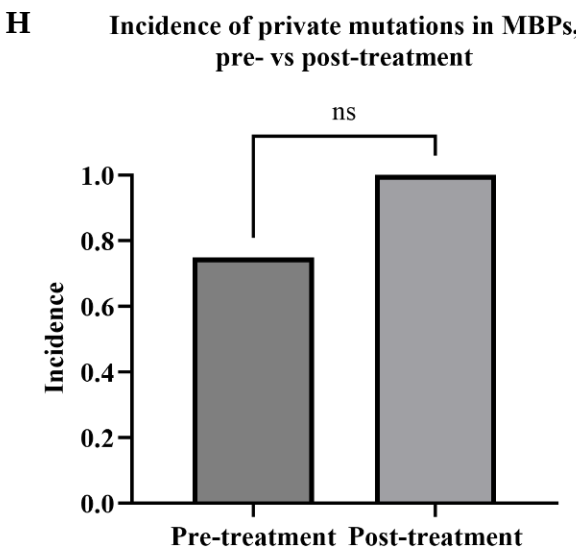

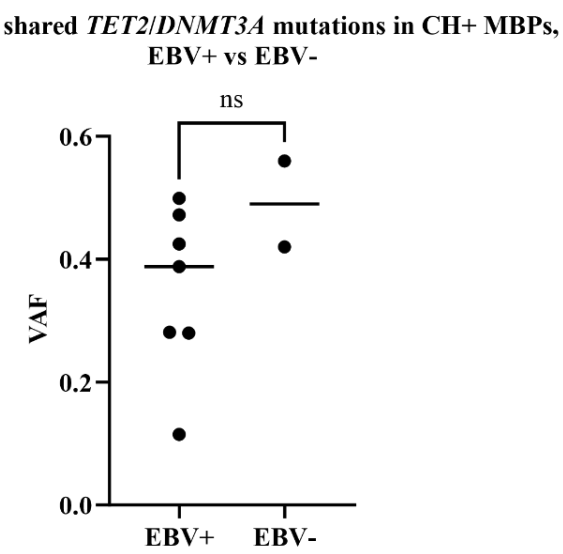

Supplemental Figure 1, Continued

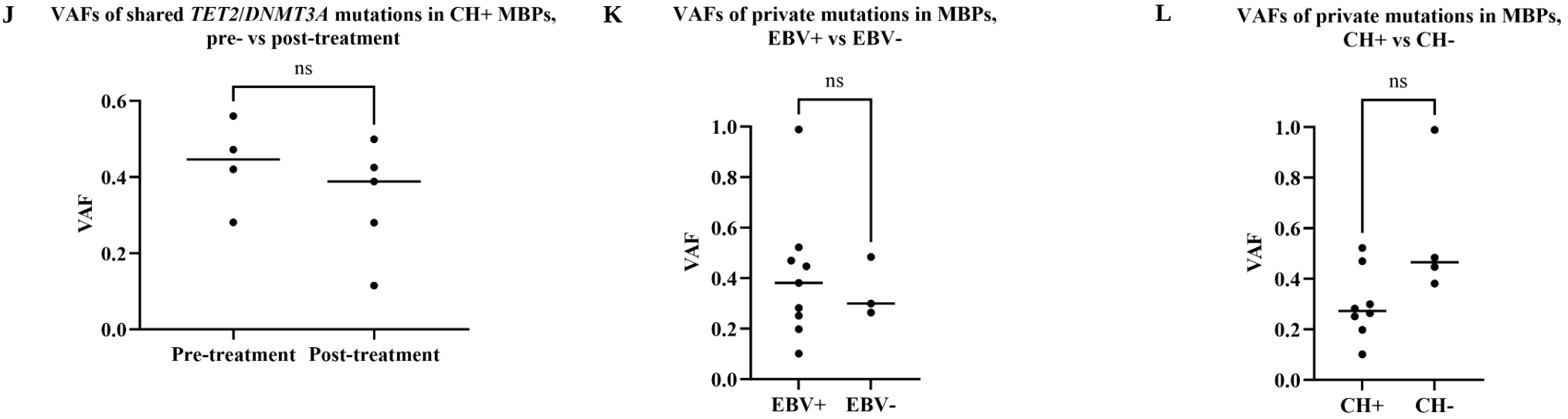

Supplemental Figure 1. Comparisons of the incidences and allele frequencies of shared and/or private mutations in polytypic B cells and monotypic/monoclonal B cell proliferations among various groups. (A) The proportion of patients with shared mutations in polytypic B cells **(**PolyBCs) and follicular helper T-cell lymphomas (TFHLs) was not significantly different among Epstein-Barr virus-positive (EBV+) and EBV-negative (EBV-) patients or (B) among those with PolyBCs sampled pre- and post-treatment. (C) The allele frequencies (VAFs) of the *TET2*/*DNMT3A* mutations in PolyBCs did not significantly differ among EBV+ and EBV- patients harboring those mutations. (D) A trend towards lower VAFs was present among samples obtained pre-treatment. (E) The incidence of shared mutations in monotypic/monoclonal B cell proliferations (MBPs) and TFHLs did not significantly differ among EBV+ and EBV- MBPs or (F) among MBP samples obtained pre- and post-treatment. (G, H) The incidence of private mutations in MBPs also did not differ among these groups. (I) Among clonal hematopoiesis-positive (CH+) MBPs (those that shared mutations with corresponding TFHLs), no significant difference in VAFs of the shared *TET2*/*DNMT3A* mutations was seen among EBV+ and EBV- MBPs or (J) among pre- and post-treatment samples. (K) Private mutant VAFs in MBPs did not significantly differ among EBV+ and EBV- cases or (L) among CH+ and CH-negative (CH-) MBPs. Horizontal lines in (C-D) and (I-L) indicate medians; ns, not significant.

Supplemental Figure 2

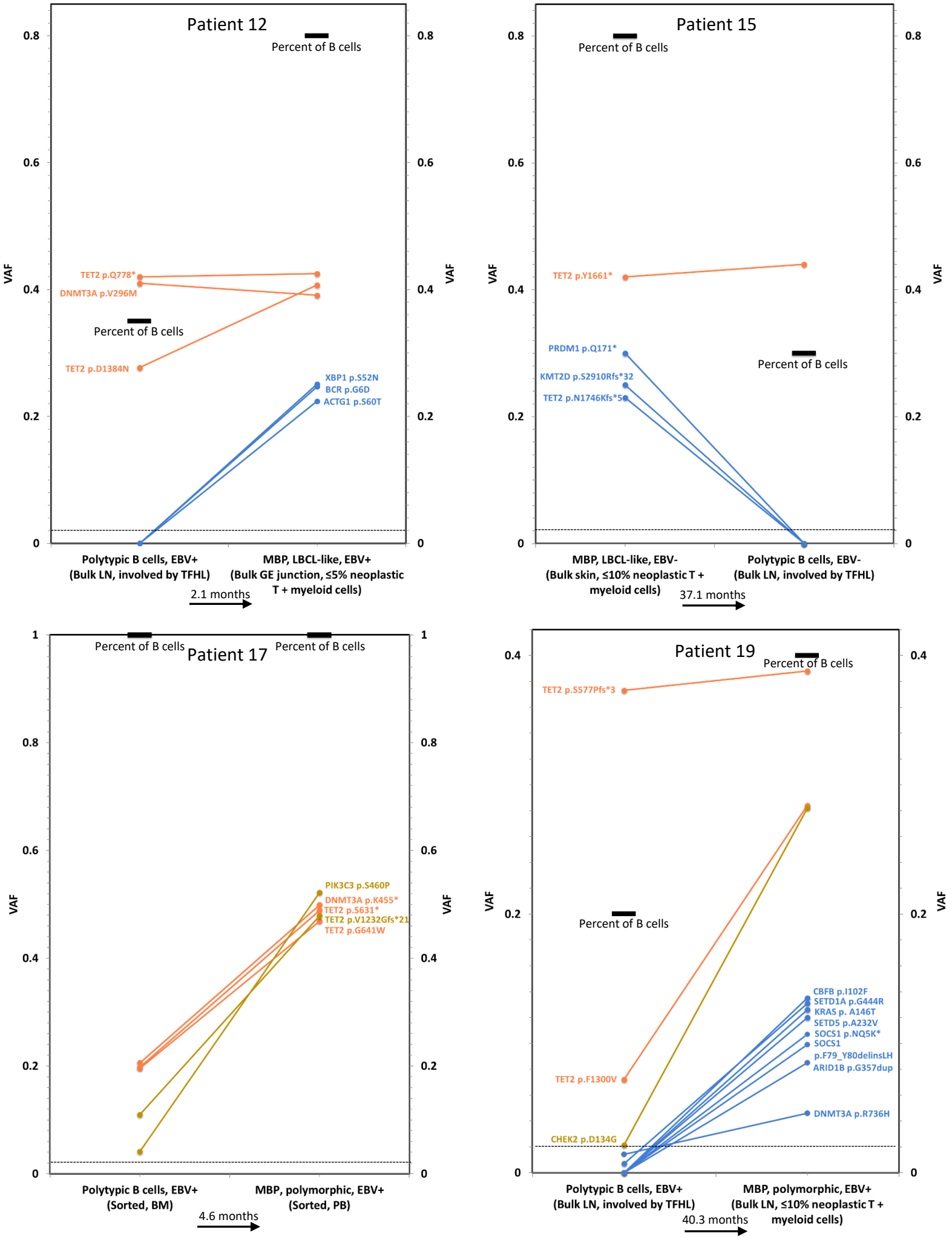

Supplemental Figure 2, Continued

Supplemental Figure 2. Comparison of mutations detected in samples containing high levels of polytypic B cells and monotypic/monoclonal B cell proliferations obtained from the same patients. Separate samples containing high levels of polytypic B cells (PolyBCs) from 4 monotypic/monoclonal B cell proliferation (MBP) patients (12, 15, 17, 19) were sequenced. Such samples consisted of lymph node (LN) involved by follicular helper T-cell lymphoma (TFHL) (patients 12, 15, 19) or bone marrow (BM) (patient 17), which either pre-dated (patients 12, 17, 19) or followed (patient 15) MBP development at time intervals ranging from 2.1 to 40.3 months. Each patient received interval systemic therapy in-between the PolyBC- and MBP-containing samples. At PolyBC sampling, 3 patients were Epstein-Barr virus-positive (EBV+) (patients 12, 17, 19) and 1 EBV-negative (EBV-) (patient 15), the same EBV status as each patient's corresponding MBP. As the samples containing PolyBCs from patients 12, 15, and 19 were sequenced in bulk, determination of whether the shared mutations were present in the PolyBCs could not be performed. However, the private mutations seen in the corresponding MBPs were not identified despite high levels of PolyBCs in these samples. The *CHECK2* mutation in patient 19's PolyBC-containing sample was present at a low allele frequency (VAF) just below our cutoff (0.02) and whether it was present in background myeloid cells or in the PolyBCs could not be determined in this bulk sample. The PolyBCs from patient 17 were flow cytometry-sorted and harbored both the shared and private mutations detected in the MBP but at significantly lower VAFs. The PolyBC sample predated the MBP sample by a short time interval (4.6 months) in this case. The Y axes indicate the VAFs of the mutations detected as well as the fraction of B cells among total cells in each sample (horizonal black bars). The sample descriptions (including tissue site, EBV status, flow cytometry sorted vs bulk, and degree of involvement by other cell types) are indicated on the X axes with the time in-between the samples indicated on the bottom. Dotted lines indicate the VAF cut off of >0.02 used in this study for variant calling. Mutations in orange indicate those shared among the MBPs, TFHLs, and myeloid compartments, those in blue indicate private mutations found in MBPs and not in corresponding TFHLs or myeloid cells, while those in yellow indicate mutations detected in MBPs and myeloid cells but not in TFHLs. Private mutations detected in the TFHLs are not displayed. GE indicates gastroesophageal; LBCL, large B-cell lymphoma; PB, peripheral blood.